Journal of Applied Geophysics 150 (2018) 208–229

Contents lists available at ScienceDirect

Journal of Applied Geophysics

journal homepage: www.elsevier.com/locate/jappgeo

Applying TM-polarization geoelectric exploration for study of low-contrast three-dimensional targets

Arkadiy Zlobinskiy [a,*], Vladimir Mogilatov [b], Roman Shishmarev [c]

[a] STC ZaVeT-GEO, Novosibirsk, Russia
[b] Novosibirsk State University and Institute of Petroleum Geology and Geophysics, Novosibirsk, Russia
[c] NIGP PJSC ALROSA, Mirny, Republic of Sakha (Yakutia), Russia

ARTICLE INFO

Article history:
Received 5 April 2017
Received in revised form 17 January 2018
Accepted 19 January 2018

Keywords:
Electrical prospecting
TM polarization
Circular electric dipole (CED)
Vertical electric current soundings (VECS)

ABSTRACT

With using new field and theoretical data, it has been shown that applying the electromagnetic field of transverse magnetic (TM) polarization will give new opportunities for electrical prospecting by the method of transient processes. Only applying a pure field of the TM polarization permits poor three-dimensional objects (required metalliferous deposits) to be revealed in a host horizontally-layered medium. This position has good theoretical grounds. There is given the description of the transient electromagnetic method, that uses only the TM polarization field. The pure TM mode is excited by a special source, which is termed as a circular electric dipole (CED). The results of three-dimensional simulation (by the method of finite elements) are discussed for three real geological situations for which applying electromagnetic fields of transverse electric (TE) and transverse magnetic (TM) polarizations are compared. It has been shown that applying the TE mode gives no positive results, while applying the TM polarization field permits the problem to be tackled. Finally, the results of field works are offered, which showed inefficiency of application of the classical TEM method, whereas in contrast, applying the field of TM polarization makes it easy to identify the target.

1. Introduction

During the last years, there have been significant changes in technologies of electrical exploration. More complex source-receiver systems are used. Three-dimensional approaches to interpretation are utilized. Finally, the methods of representation (visualization) of field data and interpretation results are progressively complicated. When surveying a geophysical environment, all the tendencies mentioned above are of great importance for increasing utility of geoelectric prospecting, but the main applying this electrical method is still investigation of near-surface, well-conducting targets (ore deposits, water horizons, and etc.) in a non-conductive host medium.

We consider that it is possible to find new problems for electrical exploration and to extend its applicability area. In order to extend significantly capabilities of electrical exploration, we propose to give consideration of optimization of an electromagnetic field source and applying the electromagnetic field only TM polarization without influence of the TE polarization field. The transient methods of electric prospecting use the conventional loop as a source of the pure TE field and the horizontal electric line as a source of the mainly TE polarization field. For excitation of a pure electromagnetic field of the TM polarization, such land-based source as circular electric dipole (CED) is proposed to be used. The description of this source is given below when the method will be presented. Using the electromagnetic TM polarization field, we get an opportunity to study targets (including nonconductive ones) that are less contrast as compared to the host medium, to increase the depth of targets under study, to decrease the distance between measurement points, and, in such case, to single out targets by their change in resistivity and polarization parameters.

Practical application of the TM field is worthy also in studying conductive targets in non-conducting media (wherein TE electrical explorations are actively applied). We don't focus attention on this fact because until the time as there exists at least illusive hope to obtain a result with using a loop or a horizontal current line, geophysicists will use these sources as a habitual, although often ineffective tool for performance of operations.

2. Electromagnetic fields of TE and TM polarizations

Separation of an electromagnetic field into TM and TE modes is possible in a one-dimensional horizontally-layered medium.

It should be recalled that the TM mode (or the field of the electric type) does not have a vertical magnetic component and the TE mode does not have a vertical electrical component (the field of the magnetic

* Corresponding author.
E-mail addresses: office@geozvt.ru (A. Zlobinskiy), ShishmarevRA@alrosa.ru (R. Shishmarev).

https://doi.org/10.1016/j.jappgeo.2018.01.020
0926-9851/

type). Thus, fields of both TE- and TM-polarizations are orthogonal to each other. Separation of the electromagnetic field into fields of TE and TM polarization is informal because these components of the general field have different space-time characteristics and physical properties. A source of a field of only the TE polarization is known and it has long being used in electric prospecting and such source is the ungrounded loop. The source generating only the TM-polarization field is less known, although it was proposed away back in the nineties (Mogilatov, 1996) and it is the circular electric dipole (CED).

It is of interest that CED, on the other hand, can be considered as a land countertype of vertical electric current line arranged in a borehole or in sea. This was discussed in rather detail for several times (Goldman and Mogilatov, 1978; Goldman, 1990; Mogilatov and Balashov, 1996). The patent for works with the vertical current line was obtained as early as in sixties (Nazarenko, 1962). Both the vertical current line and circular electric dipole excite a field of the electric (TM) type. However, when such a source is implemented as the vertical current line, great difficulties emerge, especially if works are intended to be carried out on land or in shallow sea, whereas applying the CED opens a new direction in controllable geoelectrics. The present-day state applying a vertical current line in a sea is considered, for example, by Helwig et al. (2013).

Fig. 1a demonstrates images of current lines for the loop as a source of only the TE polarization field. In Fig. 1b and c there are given current lines for the vertical current line and CED. Both sources generate only the TM polarization field. Currents lines for the loop are horizontal and these don't pass through boundaries of horizontal layers. For the CED, there is the opposite situation, current lines are perpendicular to loop current lines and intersect boundaries of horizontal layers. Currents generated by CED are affected not only by horizontal, but also by vertical resistivity of a medium. A special toroidal configuration of secondary current generated by CED with involvement of the vertical current component possesses phenomenal features, which are unknown and impossible in traditional transient electromagnetic sounding (TEM).

In this case, the reasonable question arises as what about the horizontal current grounded line which is often used by a source of an electromagnetic field? Indeed, the horizontal current line is a combined source. It excites fields of TE and TM polarization, which gives a hope to use properties of both TE and TM fields. In fact, it is not the case. It has been shown so long ago that when using the horizontal current line, the transient electromagnetic TM field plays a very insignificant role for late times (at great depths of investigation) as compared to that for a field of the magnetic type (TE).

It should be recalled the main properties of an electromagnetic field of the TE polarization usually used in geoelectrics. The renowned "smoke current ring" described by Nabighian (1979) that is generated by a loop, is formed by only horizontal current lines and is characterized by a wide lateral extension. On the ground surface, we have a response defined by the all host strata. Under these conditions, study of weak anomalies faces the problem of a background signal, i.e., the signal governed mainly by the horizontal medium conductivity, the information on the highly generalized conductivity distribution being available. The unsolved problem of removal of a background that is typical for conventional electrical surveys on technology of transient electromagnetic soundings (TEM) is not at all a technical problem, but it is the high-priority one related to a source of electromagnetic field. Within this framework, manifestation of any other electromagnetic parameters of a medium except conductivity, as well as of the fine structure of the conductivity distribution is subtle. It may be said that the TE field is "rough" instrument of geoelectric surveying. Alternatively, a field of the electric type may be used.

3. Method of vertical electric current soundings (VECS)

Before the appearance of CED, there were no practical ways for surface excitation of a transient field of the only electric type (TM polarization), and using a vertical current line was limited in consequence of great problems of source realization. In light of this, the overwhelming scope of surveying the transient geoelectrics in the world is pertinent to the problems of interaction of a geologic medium with a TE polarization field and, that is the saddest, geoscientists are not aware of unilateral embracement and limitations of such works. Accordingly, this situation is supported by a field practice where methods based exceptionally on applying a field of the magnetic type are used. Unfortunately, such unilateral embracement is perceived as unavoidable reality in monographs and guidebooks on electromagnetic methods. We hope to extend thoughts of geophysicists about possibilities of electromagnetic methods. The basic information on VECS is given by Mogilatov et al. (2016, 2017). Some basic VECS aspects were described earlier by Helwig et al. (2010) and by Mogilatov et al. (2009). A series of articles concerning application of VECS in sea and in the Arctic region were recently published (Goldman et al., 2015; Haroon et al., 2016; Mogilatov et al., 2016, 2017). Articles describing examples of applying VECS for delineation oil deposits (Balashov et al., 2011), for ore deposits (Zlobinskiy and Mogilatov, 2014), as well as description of basic VECS principles (Mogilatov, 2014) were published in Russian. VECS can use for analysis of IP parameters. Analysis of IP parameters at TE polarization field were published (Park et al., 2017; Seidel and Tezkan, 2017).

By the method of vertical electric current soundings (VECS) we mean such geoelectric investigations, which are performed making use of a circular electric dipole (CED) as a source of the electromagnetic field. The CED geometry is formed by several grounded radial horizontal lines (usually 8) into which pulse current of the same form and amplitude is supplied simultaneously. Measurements are performed throughout an arbitrary grid around a field source (at the large CED radius and inside the source) with the aim to record a dense areal transient signal (of three-dimensional data cube). A rate of magnetic induction is usually measured with the help of compact inductive pickups. Lately, measurements of an electric field by grounded receiver lines are of the great interest. The surveying scheme is shown in Fig. 2.

Prior to measurements, a current circuit CED is mounted. The source radius is appropriate to the depth and area of investigations. For the most of rocks surveys, the radius is governed by the area being studied. Qualitative measurements are usually performed at a distance up to 5 CED radii, although there were areas in our practice on which we successfully carried out measurements at the distance of 6–7 radii from the CED. The geometry of a source is meant to be corresponding to the project of CED and currents in lines are equalized, the currents

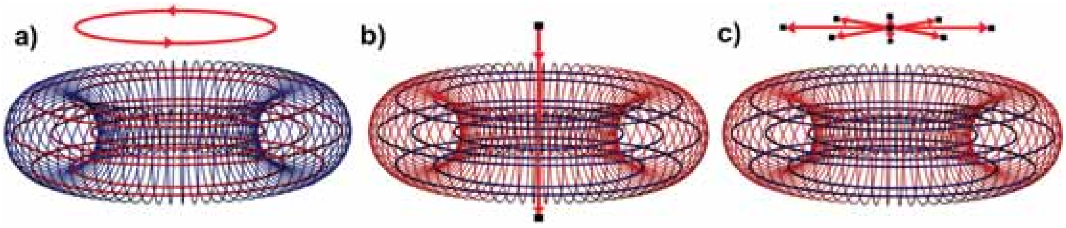

Fig. 1. Current lines generated in ground by the a) loop, b) vertical line, c) CED are displayed by red color. Magnetic field is displayed by blue color.

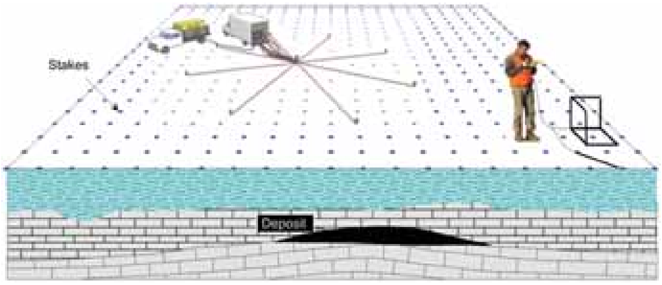

Fig. 2. Generalized scheme of surveying by VECS method.

being in the pulse mode. It is the automatic system for maintenance of equal currents in lines that is specific VECS equipment. Depending on posed problems, each measuring group is equipped by one or several devices measuring a transient signal, such group can operate with one or several inductive pickups and measuring ground lines. All receiving components such as pickups, measuring lines, devices measuring a transient signal are standard elements applied in the method of transient processes (TEM or TDEM). Each of groups with its own measuring set can freely move over an area using space-time satellite navigation to locate the field source. Thus, if the standard distance of five radii from the center of CED source is taken for maximum distance, then the area of ~25 km^2 may be surveyed efficiently at a fixed source of 0.5 km radius.

If we proceed from the insight about the field of arbitrary source as a superposition of fields with TM and TE polarization, then CED excites a transient TM field in the ground (in contrast to a loop and horizontal line, which excite either pure, or mainly TE field). When the CED excites a horizontally-layered medium on a ground, there is no magnetic field. This is the most important property for practical applying in electrical exploration. Since a response from a host medium is absent, then the presence of a signal itself indicates the presence of a three-dimensional disturbance in the host medium and characteristics of this signal are governed by properties of both the target and host medium. This signal from the heterogeneity is well-localized, i.e., the source of the signal being measured is located under the measurement point of a magnetic field. As a consequence of this is the fact that the influence of other heterogeneities located between the transmitter and receiver of the field is significantly weakened. Exception may be due to strong heterogeneities located immediately near the source and its electrodes. This situation leads to appearance of a background over the all surveyed area. Such cases have occurred in practice. However, this background doesn't impede to single out other local targets at a distance from the transmitter just for the reason that the signal from these heterogeneities is spatially localized.

It should be noted that it is meaningless to use the 1D approach for interpretation of measurement results of field magnetic components since only the three-dimensional approach is needed. However, due to response nature related to heterogeneity, areal image of a VECS signals possess high visualization ability and these have obvious value in the perception of a customer of works. The next interesting property of a CED field is the fact that local targets-anomalies of conductivity in a signal versus the velocity of vertical magnetic induction (we call this the $\partial B_z/\partial t$ component) manifest themselves in different ways in the $\partial B_\phi/\partial t$ components. In the areal representation of the signal ($\partial B_z/\partial t$), the center of the target lies on the line of reverse of the $\partial B_z/\partial t$ component. In other words, we will determine well the center of a local target by the $\partial B_z/\partial t$ signal, and the target boundaries will be determined by the signal $\partial B_\phi/\partial t$. A useful aid is in measurement of an electrical radial gradient E_r. The E_r component is normal, i.e., it is a response of one-dimensional host medium when CED is used as a source. Nevertheless, the signal nature is sharply changed when a local target is located in a horizontally-layered medium. The sharp change in the E_r nature coincides with the target boundary nearest to CED.

Note one more property of the CED field as opposed to fields of conventional loop and horizontal current line: operations with CED suggest a dense survey grid, just this grid makes sense. When operations are carried out by the VECS method, a signal is changed rather faster when passing from point to point since the signal characterizes mainly a medium under a measurement point rather than average medium between a source and receiver.

Interpretation in the VECS method is performed with another approach than in those “classical” methods where the main portion of a signal accounts for the contribution of a host medium. For the ‘classical’ method, various, sometimes rather complex, procedures for removal of unnecessary (but prevailing) contribution due to a host medium are well developed. We don't need to do this. We have done everything necessary at the stage of development of a complicated source that optimizes response at the physical level. When processing, it is too late sometimes to optimize. At the first stage, our principal interpretation method is plotting maps of signal distribution. But this signal reflects directly heterogeneities and provides a contour. This corresponds to maps of an anomalous signal, which are obtained after the complex processing the resultant signal in the traditional electric exploration. These maps of signals, transformed into some apparent resistivities, are often taken as the final result. In addition to this, we suggest three-dimensional visualization of the target directly according to the field data and fitted by direct three-dimensional simulation.

4. Comparison of applicability of the classical TEM with VECS based on three-dimensional numerical simulation

4.1. Model 1. Kimberlite pipe in Yakutia

The 3D program GeoPrep was used for calculations VECS signals. The finite element method is used in the program (Persova et al., 2011). The program GeoPrep is used in many organizations in Russia and was compared with different 3D programs many times. Calculations for loops transmitter were conducted for the three-dimensional model applying the Podbor program. Calculations of 3D models in the Podbor program are based on the Born approximation. Podbor program was tested by the program GeoPrep.

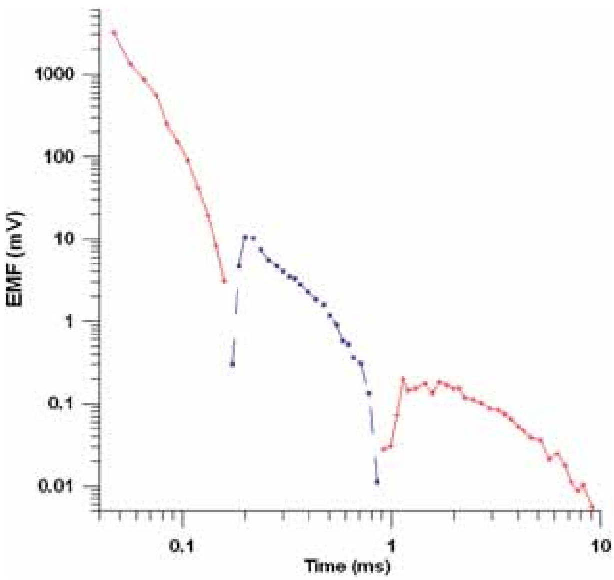

Fig. 3. E.m.f. measured in Yakutia when operating with square loop with side 100 m. The positive signal is shown as red crosses and the negative signal is shown as blue circles.

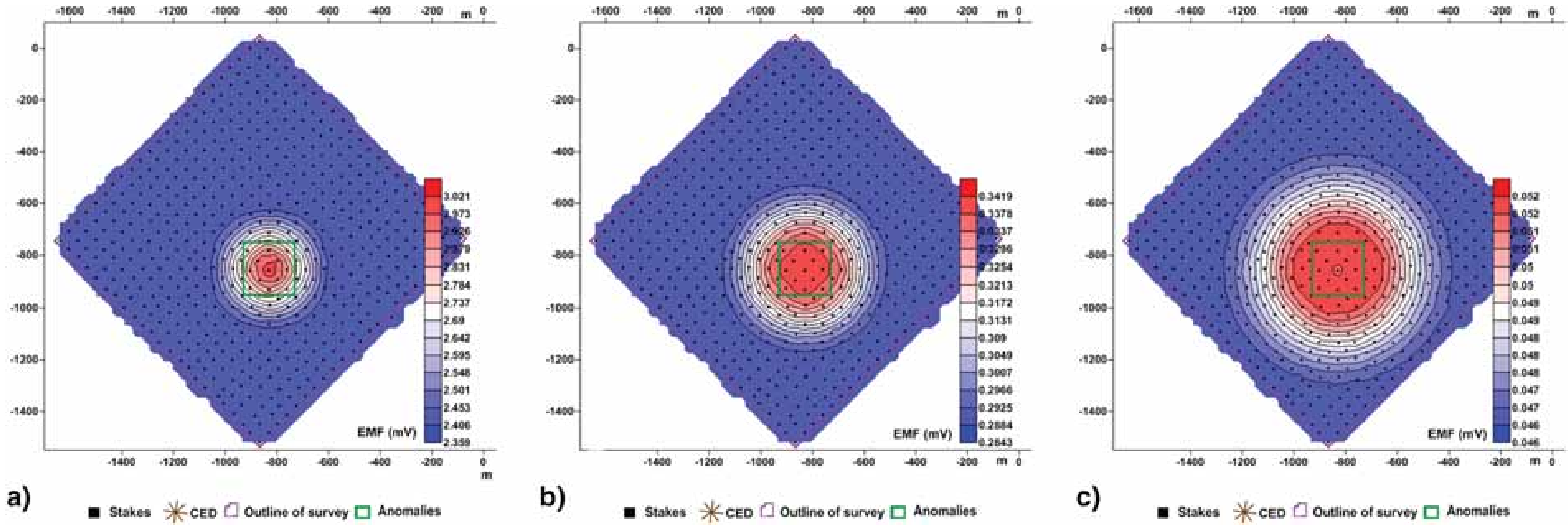

Fig. 4. Areal of transient electromagnetic TEM signals (e.m.f.) distribution for the model 1. Times a) 0.216 ms, b) 0.508 ms, c) 1.058 ms.

The TM field possesses a series of properties unusual for the classical electrical exploration by TE field. When surveying low-contrast targets, we are primarily interested in influence of the slight change of medium resistivity on a signal being measured and localization of this change. One example of such type of problems on localization of three-dimensional low-contrast targets is distinguishing kimberlite pipes on the grounds of the Republic Sakha (Yakutia), Russia.

For searches of kimberlite pipes under conditions of Yakutia, the following problems are characteristic when electrical exploration methods are applied:

1) Targets are low-contrast for electrical exploration by applying TE field. The horizontal resistivity of a host medium and that of kimberlite bodies are slightly different and sometimes the resistivity of kimberlite bodies is quite within the range of the host medium resistivity.
2) Near-surface targets are most frequently studied, but presently customers are interested in targets overlying by sediments with 100 m and more in thickness.
3) Permafrost and, as a consequence, the presence of ice almost in all rocks generate processes of fast induced polarization. The induced polarization significantly complicates interpretation of data acquired during electrical exploration. The most common kind of electrical exploration in Yakutia is surveying with the ungrounded loop for excitation of the electromagnetic field and measurement of the $\partial B_z/\partial t$ component at the center of a square loop. The length of the source sides is most often 50–100 m. When such configuration with such loop sizes is used, fast IP processes significantly distort the measured signal that forces geophysical companies to conduct additional measurements with moving receiver loops out from the transmitter loop. Given in Fig. 3 is the characteristic curve measured in Yakutia. The positive signal is displayed by red crosses and the negative signal is displayed by blue cycles. We can see that the curve is strongly complicated by IP processes. There are two zero-crossings at times 0.15 and 0.8 ms. Measurements of the signal were performed by a pick-up with the side 1 m and the effective area 10,000 m^2 located at the center of a square loop with the 100 m side.

Let us model a representative problem of localization of a kimberlite pipe applying the classical electrical exploration. When surveying is conducted in Republic Sakha, Yakutia, the common problem is distinguishing a kimberlite pipe with the resistivity 40 Ω∗m against the background of a host medium with the resistivity 70 Ω∗m. Consider a pipe with diameter of 200 m. The pipe is overlain by the strata 60 m thick. The kimberlite pipe is implied to be in the form of parallelepiped with the resistivity 40 Ω∗m situated in a half-space with the resistivity 70 Ω∗m. The target sizes in ground plane are 200 × 200 m, the depth of cover is 60 m, and the target thickness is 440 m. Target angles have the following coordinates: X1 = −930, Y1 = −750; X2 = −730, Y2 = −750; X3 = −730, Y3 = −950; X4 = −930, and Y4 = −950. The site of works is a square with sides of 1100 m. Measurements are carried out throughout a rectangular grid with 50 m-distance between measurement points. There are used 23 lines, each having 23 measuring points, i.e., 529 measuring points in total. Calculations are performed for square loops 50 m on side. That is, we need to set 529 sources of electromagnetic field for operating. The current in a loop is 10 A and the effective pickup area is 2500 m^2. The measurement accuracy under conditions of low noise is 1 μV. We focus on parameters of the equipment widely used in Yakutia when surveying by the transient electromagnetic method.

The calculation results for such model at times a) 216 μs, b) 508 μs and c) 1058 μs are given in Fig. 4. Calculations were conducted for the three-dimensional model applying the Podbor program. Calculations of 3D models in the Podbor program are based on the Born approximation. Fig. 4 demonstrates color scales for each time: the values of e.m.f in mV. Fig. 5 presents the results of calculations transformed into apparent resistivity values and the model of the pipe used in the calculations. Red squares visualize the kimberlite pipe model, dark-grey surface visualizes an apparent resistivity with the value 65 Ω∗m.

What do the calculations indicate? The signal exceeds the level of 1 μV before 5 ms time. Maximum deviation of a signal from the reference signal is recorded over the anomaly center at time 216 μs, the deviation is 28%, and the apparent resistivity value is decreased to 61 Ω∗m. Such values are recorded only at a single measurement point over the model center. When real works are carried out, anomalies recognized only at one measurement point are eliminated. Because of this, it is better to take into account only the maximum deviation of 22% at time of 216 μs and the lowest resistivity of 63 Ω∗m. With increasing the time, the number of points at which the anomaly is recognized decreases. At a time 1058 μs, the anomaly accounts for less than 10%, the minimum apparent resistivity being 65 Ω∗m. This is well explained by the fact that with increasing the time, the signal being measured gives information averaged over the increasing area, therefore, the contribution of a three-dimensional target is decreased against the background of a reference medium. Such behavior of the electromagnetic field when applying a loop is well known for a long time and it has been described as early as in 1979 by Nabighian (1979). Is it possible to identify such a target when interpreting? It is possible to distinguish a target based on formal attributes inasmuch as the change in a signal exceeds the measurement accuracy of equipment. Recall that the measurement accuracy for signals more than 100 μV is usually estimated at 1%. In practice, no one will pay attention to such changes in signals. If signals are visualized at the same times using most common transformation such as apparent resistivities, then the resistivities will vary at time 216 μs from 61 Ω∗m to the reference value of 70 Ω∗m and at time of 1058 μs from 66 to 70 Ω∗m. That is, the decrease in resistivity of the reference medium to 65 Ω∗m

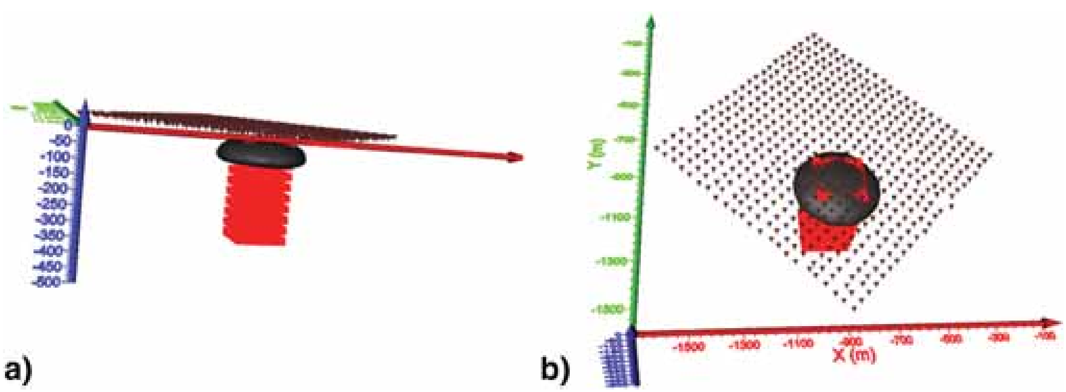

Fig. 5. Model of kimberlite pipe (red squares), dark-grey surface shows apparent resistivity value of 65 Ω∗m, and brown triangles are observation points.

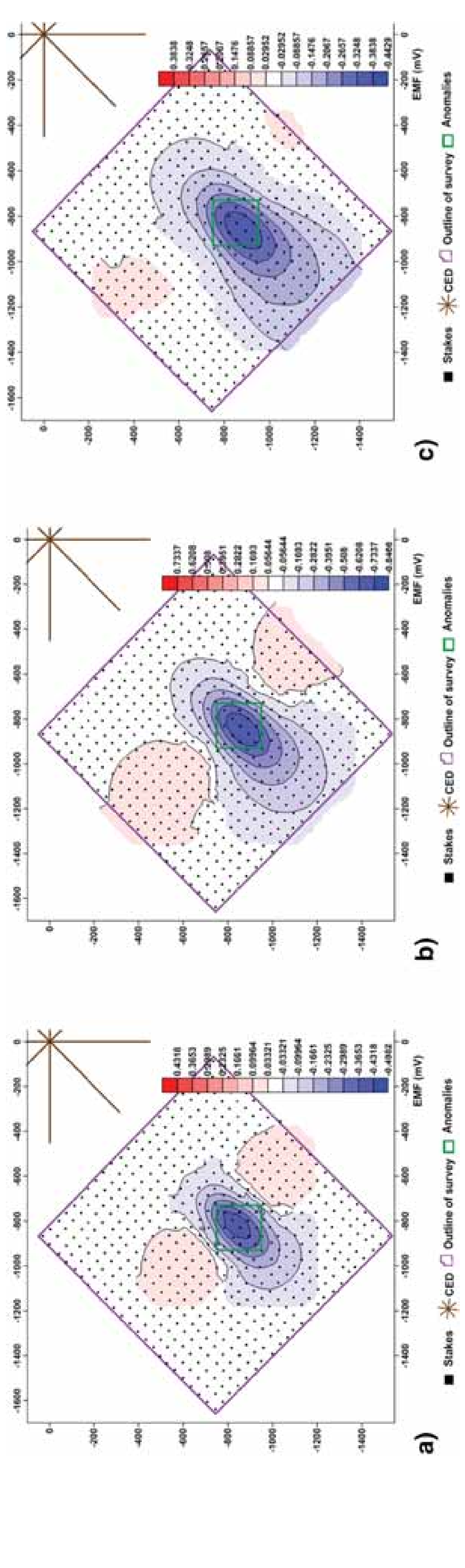

Fig. 6. Areal (normalized) distribution of $\partial B_{\varphi}/\partial t$ component of VECS signals. Times at a) 1.021 ms, b) 2.041 ms, c) 4.06 ms. VECS signal (normalized with respect to a distance from the source center) is shown.

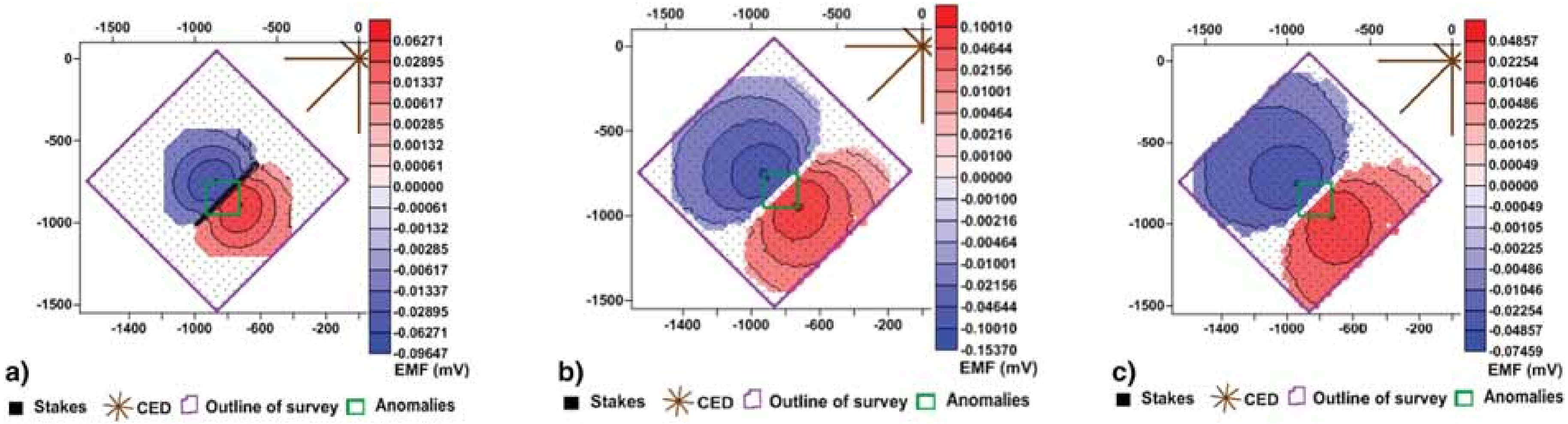

Fig. 7. Areal (normalized) distribution of $\partial B_z/\partial t$ component of VECS signals for model 1. Times at a) 1.021 ms, b) 2.041 ms, c) 4.06 ms. VECS signal (normalized with respect to a distance from the source center) is shown.

can be taken by operators as a small the deviation of resistivity of a host medium.

It should be noted in addition that in simulation of the transient electromagnetic method, we didn't make allowance for effect of IP processes, which significantly change the nature of measured curves that provided surveying even relatively large targets at the shallow depth to be an infeasible problem (Fig. 3).

Consider simulation of VECS signals. The program "GeoPrep" was used for calculations. The finite element method is used in the program (Persova et al., 2011). The model of a medium completely corresponds to the model described above. The CED of radius 450 m and full-load current of 25 A with the center at the coordinate origin will be used as a source. Pickups with the effective area of 10,000 m^2 will be used as a receiver.

Here and elsewhere, when visualizing $\partial B_\phi/\partial t$ and $\partial B_z/\partial t$ components of VECS, we will use the following normalization:

Before output of areal maps, the measured signal is normalized via the equation:

$$E_{nrm}(t) = E_{fld}(t) * (R/R_{CED})^q \quad (1)$$

where $E_{nrm}(t)$ is normalized e.m.f., $E_{fld}(t)$ is measured e.m.f., R is the distance from a measurement point to the CED center, and R_{CED} is the CED radius, q is from 1 to 2.5.

Note another important circumstance: when signals are visualized, modules of the maximum and minimum values of a color scale are always equal.

Fig. 6 visualizes the distribution of the $\partial B_\phi/\partial t$ components at times a) 1.021 ms, b) 2.041 ms and c) 4.06 ms. Given in Fig. 7 is the distribution of $\partial B_z/\partial t$ component at same times. The signal distribution for both components is normalized with respect to a distance from the CED center. Fig. 8 presents the visualization of the calculation results for the $\partial B_\phi/\partial t$ components and the pipe model used in calculations. Red cubes visualize the kimberlite pipe model and dark-grey isosurface demonstrates e.m.f. (the times are transformed into depths).

What do the calculations indicate? Analyzing the areal distribution of the $\partial B_\phi/\partial t$ signal, we acknowledge that:

1) Maximum of the signal value over amplitude is over anomaly.
2) Signal maxima are displaced at various times.
3) The number of measured values exceeding the minimum measurement level is changed, but the maximum signal values with respect to amplitude are over anomaly at all times.
4) Signals vary very strongly over area up to reverse.
5) Signal is concentrated over anomaly and it has the zero value on the most part of area.

Table 1
Parameters of host medium.

	Thickness, m	ρ, Ω·m
1	700	2000
2	125	100
3	850	2000
4	275	100
5	∞	500

Analysis of areal distribution of the $\partial B_z/\partial t$ signals indicates:

1) Typical signal separation of the $\partial B_z/\partial t$ component into two symmetric parts, i.e. the positive and negative ones takes place. The symmetry line of a field passes through the center of anomaly and that of CED.
2) Signal maxima displaced at various times
3) Signals vary very strongly over area up to reverse.

The main conclusions drawn from the simulation results for this model are as follows:

1) It is impossible to single out a target applying 'classical' electrical exploration.
2) A target can be easily distinguished when a field of TM-polarization is used.

4.2. Model 2. Polymetallic deposit near Norilsk

Users of subsurface resources having sites near Norilsk are increasingly interested in targets located at great depths. This is due to the fact that the majority of near-surface targets are so far developed and that increasingly advanced techniques for ore production make such production from significant depths to be profitable. The program GeoPrep was used for calculations (the finite element method, Persova et al., 2011).

We present calculations for the model of such deposit for the methods of transient electromagnetic and VECS. For simulation, the following model of a host medium was taken (Table 1):

A target in the form of parallelepiped with dimensions 2 × 1 × 0.025 km was taken for a target object. The target was located at depths from 675 to 700 m. The target resistivity was taken to be 100 Ω∗m. The target location in a plane view relative to a source is shown in Figs. 9 and 10. The source radius was taken to be 500 m. Current of 10 A (the equipment was designed for current of 20 A) was set in a line; the total current was 80 A. The effective pickup area was 30,000 m^2. The measurement accuracy was 1 μV.

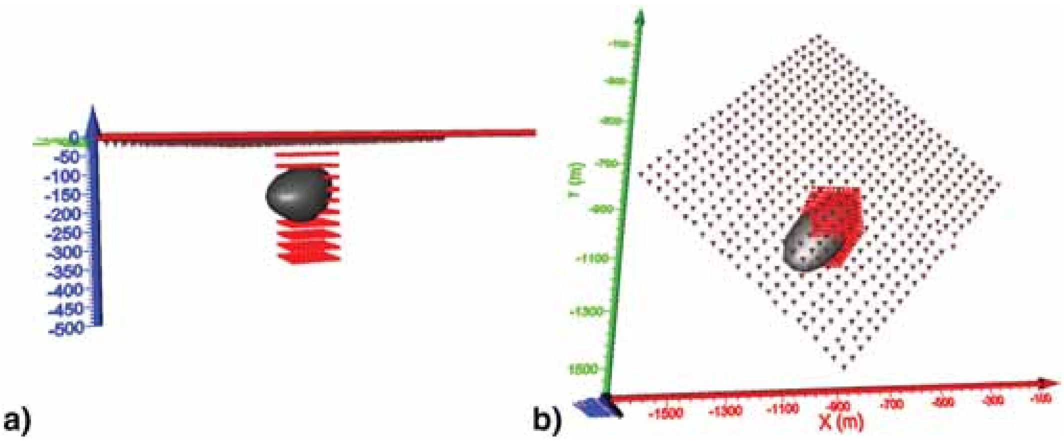

Fig. 8. Model of kimberlite pipe (red cubes) and dark-grey isosurface showing e.m.f from $\partial B_\phi/\partial t$ component.

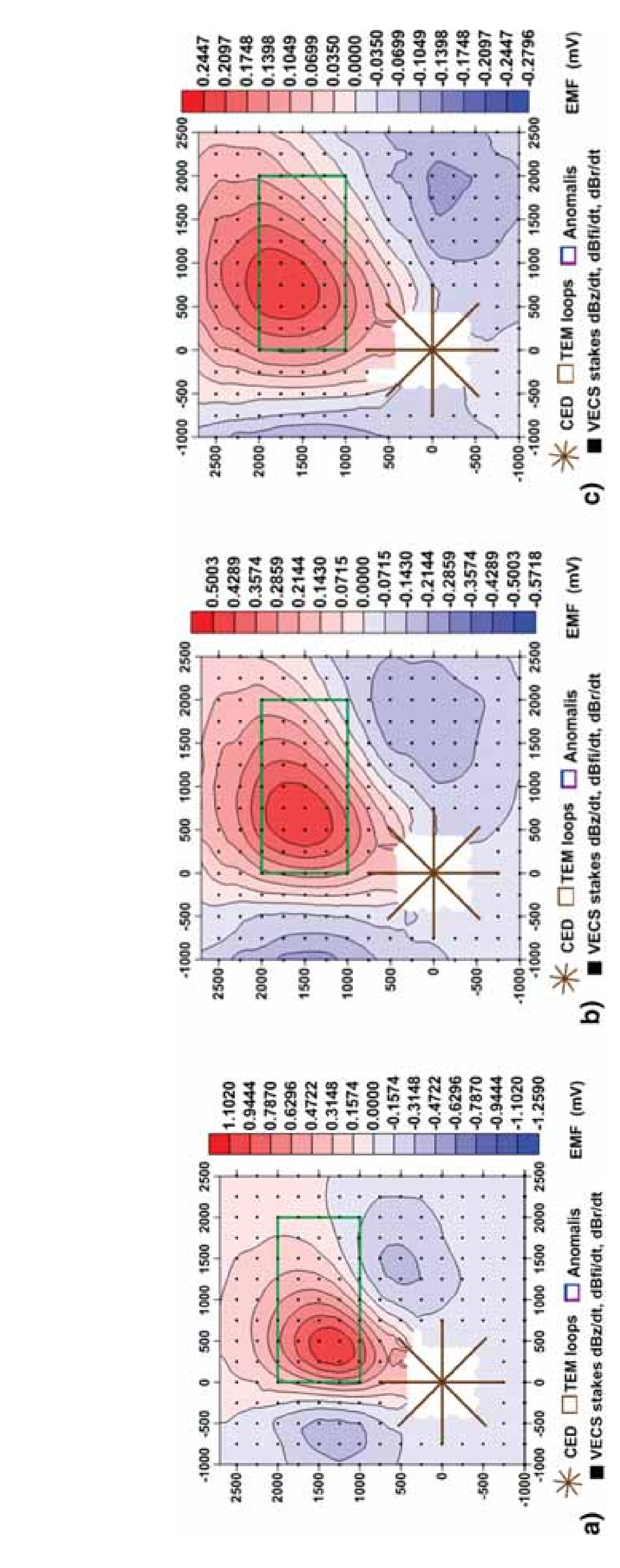

Fig. 9. Areal (normalized) calculation results for the model of the $\partial B_\phi/\partial t$ component at times a) 0.151 ms, b) 0.353 ms and c) 0.531 ms. The target under study is outlined by green rectangle.

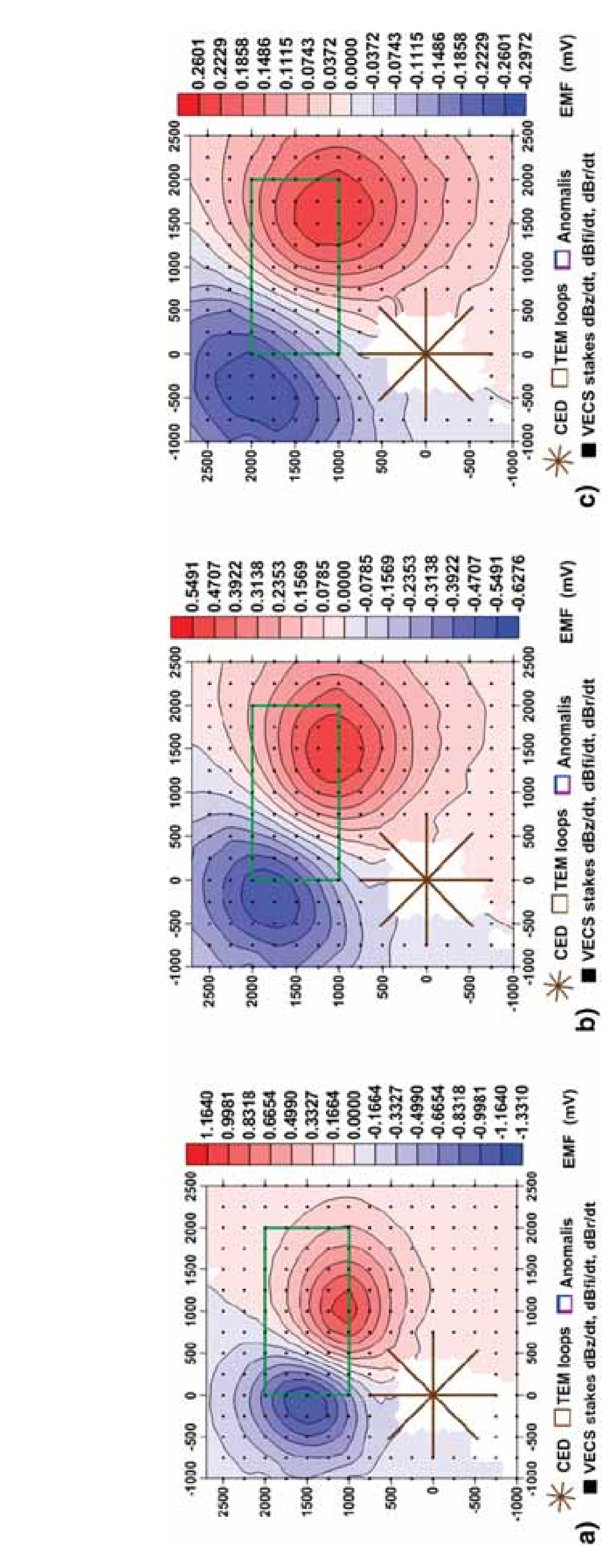

Fig. 10. Areal (normalized) calculation results for the model of the $\partial B_z/\partial t$ components at times a) 0.151 ms, b) 0.353 ms and c) 0.531 ms. The target under study is outlined by green rectangle.

Table 2
Parameters of the targets.

	X1 (m)	X2 (m)	Y1 (m)	Y2 (m)	Z1 (m)	Z2 (m)	Resistivity, Ω∗m
1	700	1700	1000	1700	−320	−300	4000
2	1300	2000	1200	2200	−460	−400	4000
3	1300	2000	1200	2200	−470	−460	50

From models offered to us, we have taken the least contrast in resistivity alternate, i.e., the version a signal for which is definitely least and it increases as the target resistivity decreases.

Fig. 9 visualizes the simulation normalized (see 1) results for the $\partial B_{\phi}/\partial t$component.

Fig. 10 visualizes the simulation normalized (see 1) results for the $\partial B_z/\partial t$component.

Conclusions derived from the simulation are as follows: the target is well distinguished by both components even at lowest resistivity contrast, well coincides with target counters, and maximum signals exceed a minimally detectable signal by 200 times.

4.3. Model 3. Polymetallic deposit with two targets near Norilsk

A host medium is assigned to be in the form of a half-space with resistivity of 1000 Ω∗m. In the medium, three targets in the form of parallelepipeds are situated. The first target simulates the presence of the upper intrusion, call it number 1. The second and third targets simulate the second, lower intrusion, call it number 2. Table 2 lists parameters of the targets. Coordinates of X and Y of the second and third targets coincide (it is the same intrusion). The Z-coordinates of the second and third targets are different (the third target is underlain by the second one), as well as their resistivities (the third target is a conducting medium). Fig. 11 demonstrates locations of mentioned targets.

First we give the simulation results for the VECS method. CED with the radius of 750 m was used as a source. The source current was 80 A. The effective area of receiver pickups was 30,000 m^2. The measurement accuracy was 1 μV. Given in Fig. 12 are measurement normalized (see Eq. (1)) results at three times 302 μs, 619 μs, and 1021 μs for the $\partial B_{\phi}/\partial t$ component. Only signals exceeding 1 μV are displayed at all times.

The calculation results show that the signal maximum of the first target is recorded at times 200–300 μs. The signal value recorded at measurement points over the first target was 30–55 μV, these signals were steadily recorded by our equipment. The maximum of a signal recorded at measurement points of the second target was recorded at times about 1000 μs. The signal value at measurement points over the second target was 15–25 μV, these signals also being steadily recorded by our equipment. At time of about 600 μs, the transient state from of a signal with prevailing contribution of the upper target to the signal with prevailing contribution from the second target was observed. Signals at times 300 μs and 1000 μs were different in signs. This is explained by the fact that, in the first case, the influence of a nonconducting target was dominant as compared with the a host medium of the first target, and influence of the conducting lower part of the second target was prevailing in the second case.

Given in Fig. 13 are the simulation normalized (see Eq. (1)) results at three times: 302 μs, 619 μs, and 1021 μs for the $\partial B_z/\partial t$ component. At measurement points related to the first target, the signal value was 30–55 μV, these signals being steadily recorded by our equipment. At measurement points related to the second target, the signal value was 15–20 μV, these signals being steadily recorded by our equipment. We

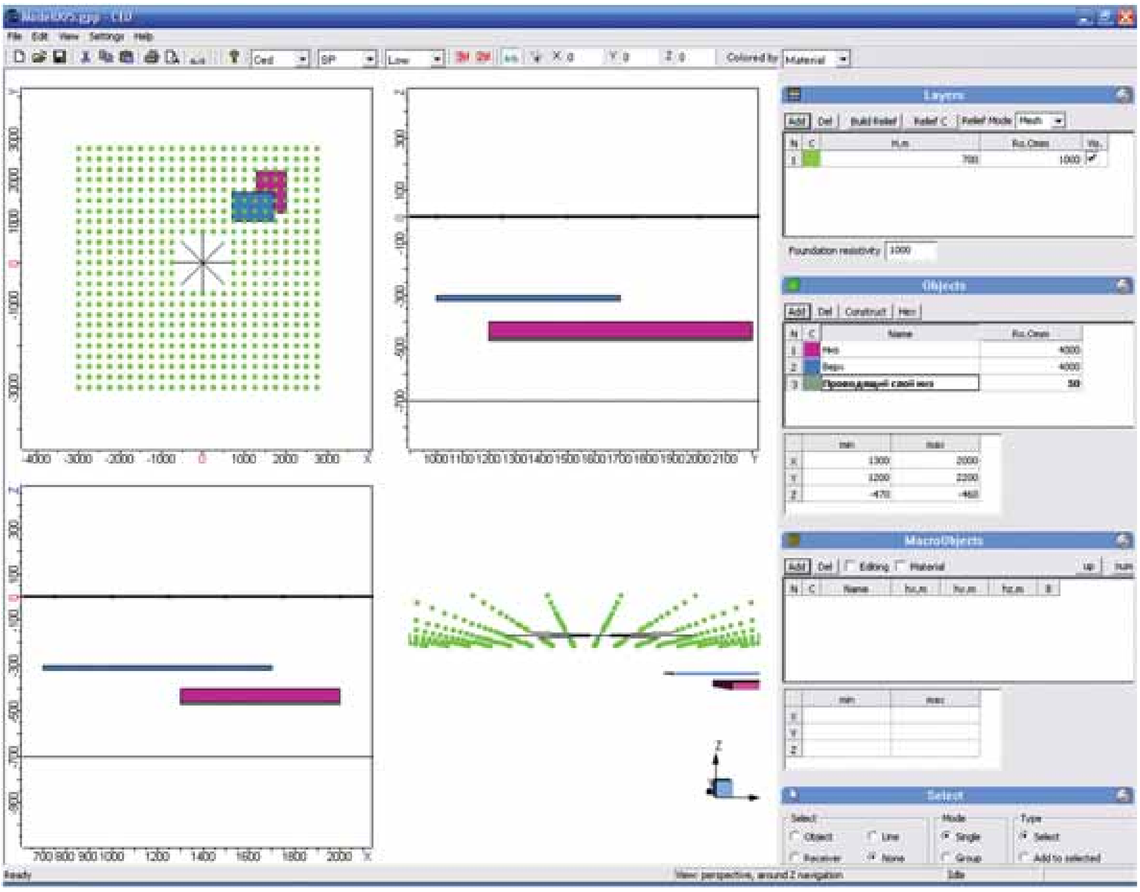

Fig. 11. Locations of targets in model 3. Blue color denotes the first target (intrusion 1), violet color denotes the second target (upper part of intrusion 2), and grey color denotes the third target (lower part of intrusion 2).

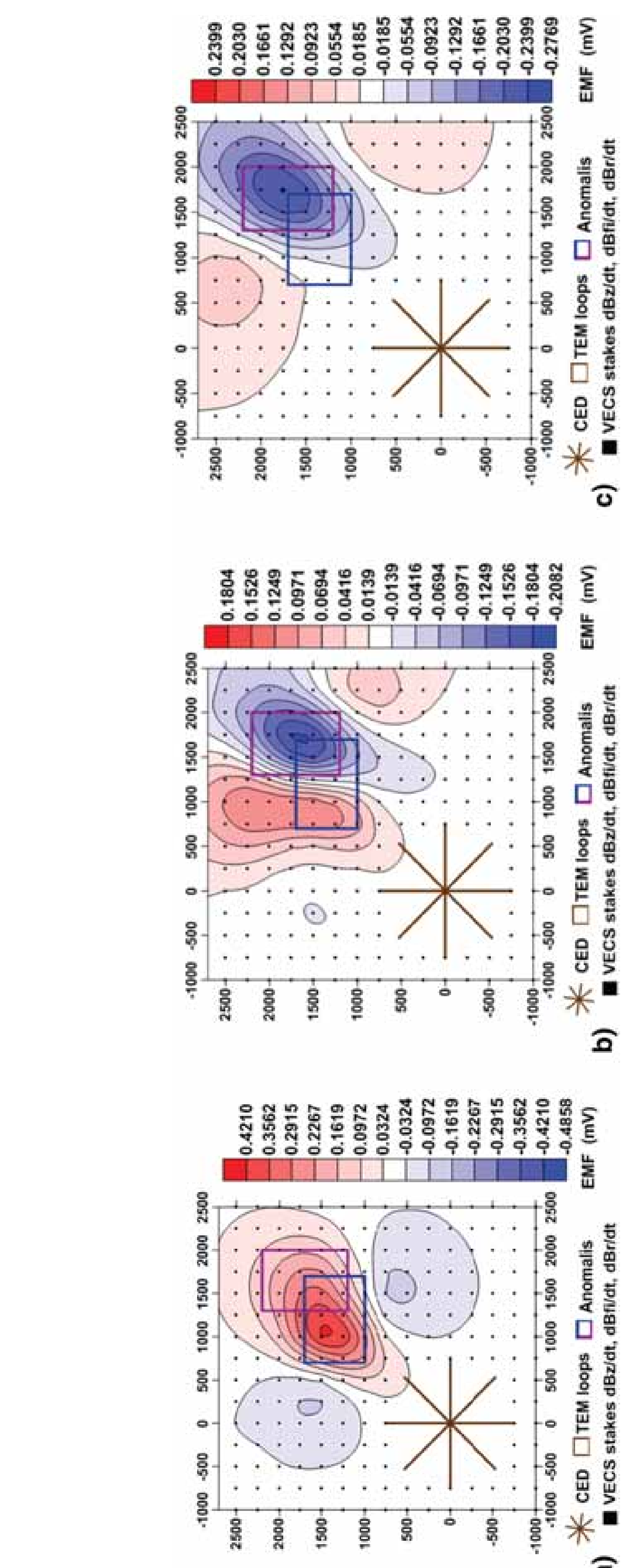

Fig. 12. Areal (normalized) calculation results for model 3. VECS method, $\partial B_\phi/\partial t$ component at times a) 302 μs, b) 619 μs and c) 1021 μs. Blue color depicts the first target (intrusion). Violet color depicts the second target (upper intrusion part).

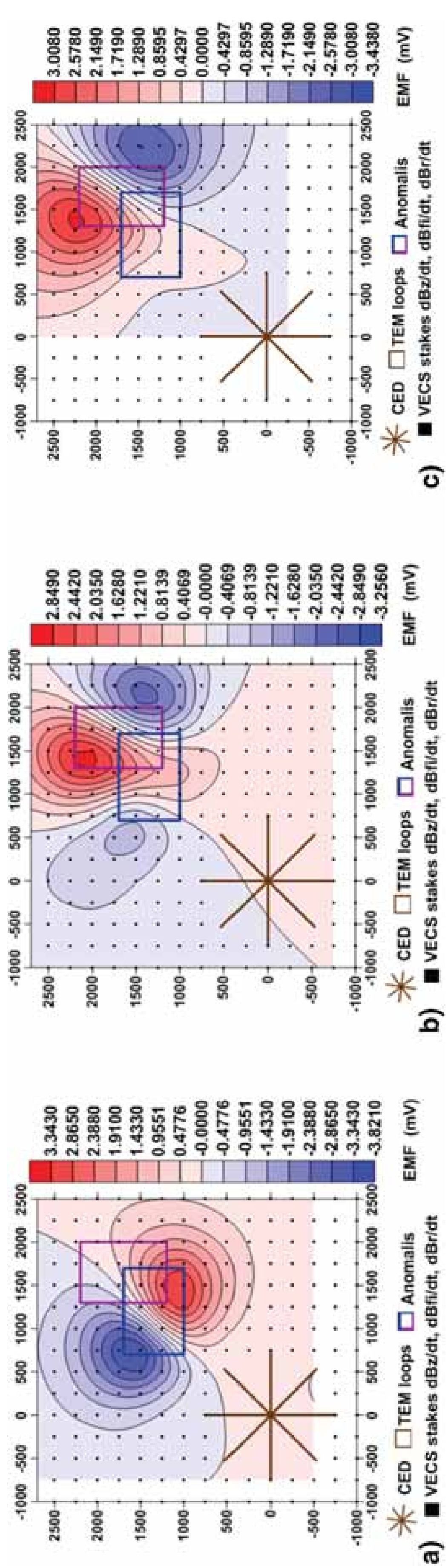

Fig. 13. Areal (normalized) calculation results for model 3. VECS method, the $\partial B_z/\partial t$ at times a) 302 μs, b) 619 μs, c) 1021 μs. Blue color depicts the first target (intrusion 1). Violet color depicts the second target (the upper part of intrusion 2).

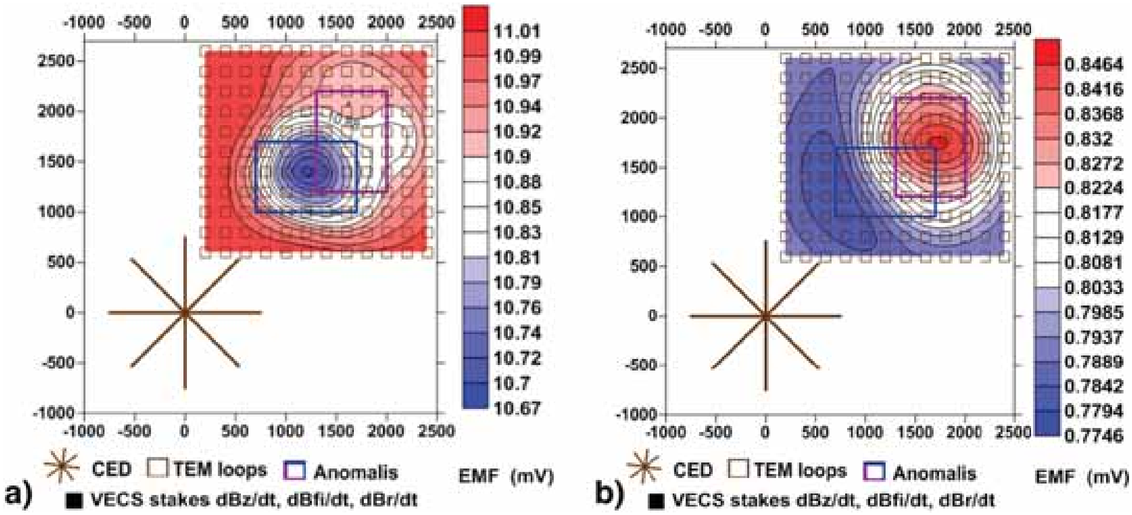

Fig. 14. Areal calculation results for model 3. The TEM signal at times a) 105 μs and b) 302 μs. Blue color depicts the first target (intrusion). Violet color depicts the second target (the upper part of intrusion 2).

note that when the $\partial B_z/\partial t$ component is measured, the sign-reverse line passes through the target center.

Now we perform calculations for the classical electrical exploration with such source as a loop. Calculations are conducted for coaxial configurations. Ungrounded loop with 100 m sides is used as a source. Receiver with effective area of 10,000 m^2 is located at the loop center. For the three-dimensional simulation of transient electromagnetic methods, the Podbor program was used. Calculations of 3D models in the Podbor program are based on the Born approximation.

We present the results of THREE-DIMENSIONAL calculations for model 3. We focus on this fact because usually, when works are substantiated, simulation of ONE-DIMENSIONAL sections is performed. The one-dimensional model has no lateral boundaries and, as a result, a study target is far more in the volume, and consequently, when one-dimensional sections are used, an anomalous signal is always greater. If one-dimensional medium were used for simulation of such situation, the anomalous signal from the first target would be 5 times more and the anomalous signal from the second target would be 6 times more.

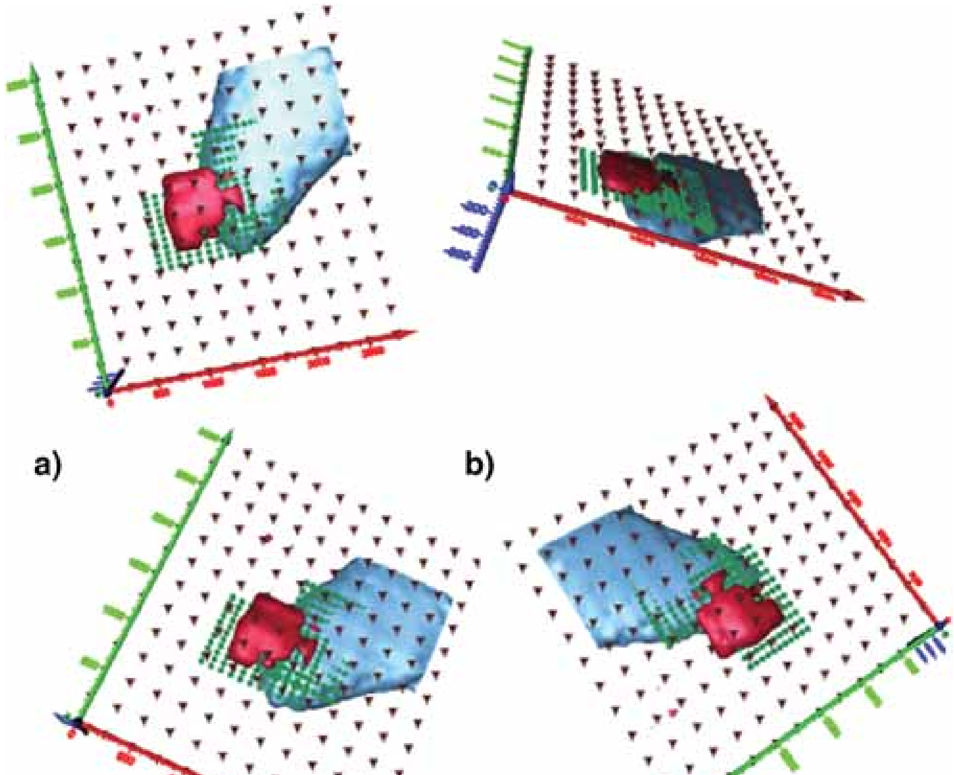

Fig. 15. Three-dimensional visualization of $\partial B_\phi/\partial t$ signal obtained due to calculation results for model 3.

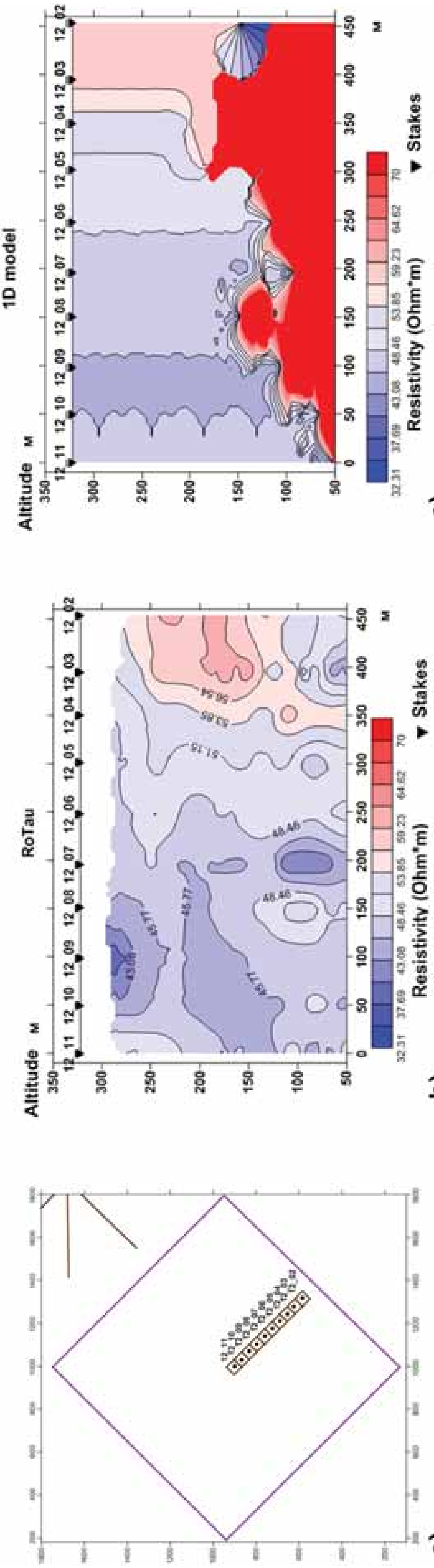

Fig. 16. a) Scheme of operation by the transient electromagnetic method. b) Apparent resistivity acquired from TEM results $\rho_\tau(z)$. c) Result of one-dimensional layer-by-layer interpretation.

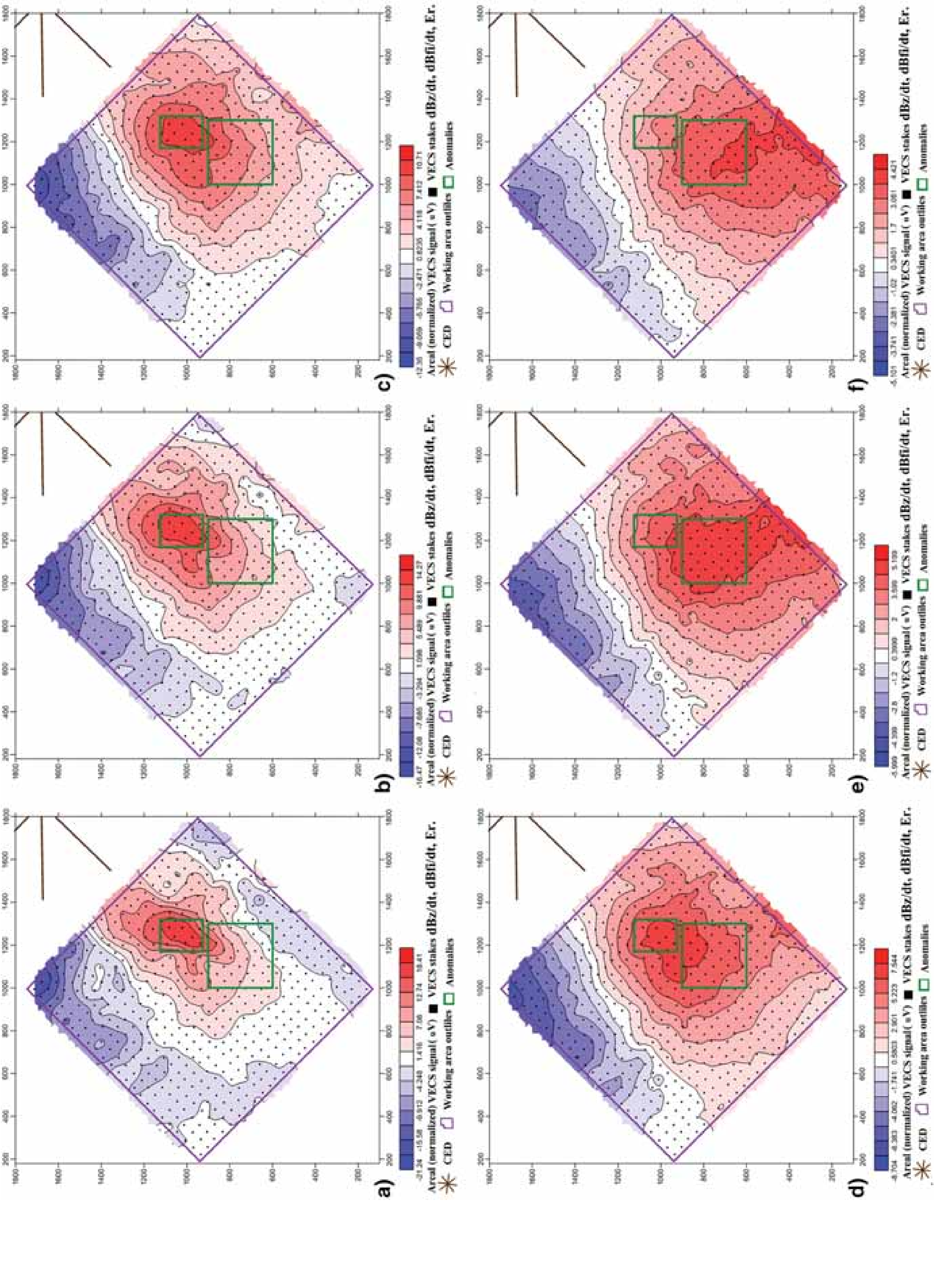

Fig. 17. Areal (normalized) measurement results of the $\partial B_\phi/\partial t$ component at times a) 0.62 ms, b) 0.849 ms, c) 1.058 ms, d) 1.565 ms, e) 1.965 ms and f) 2.429 ms.

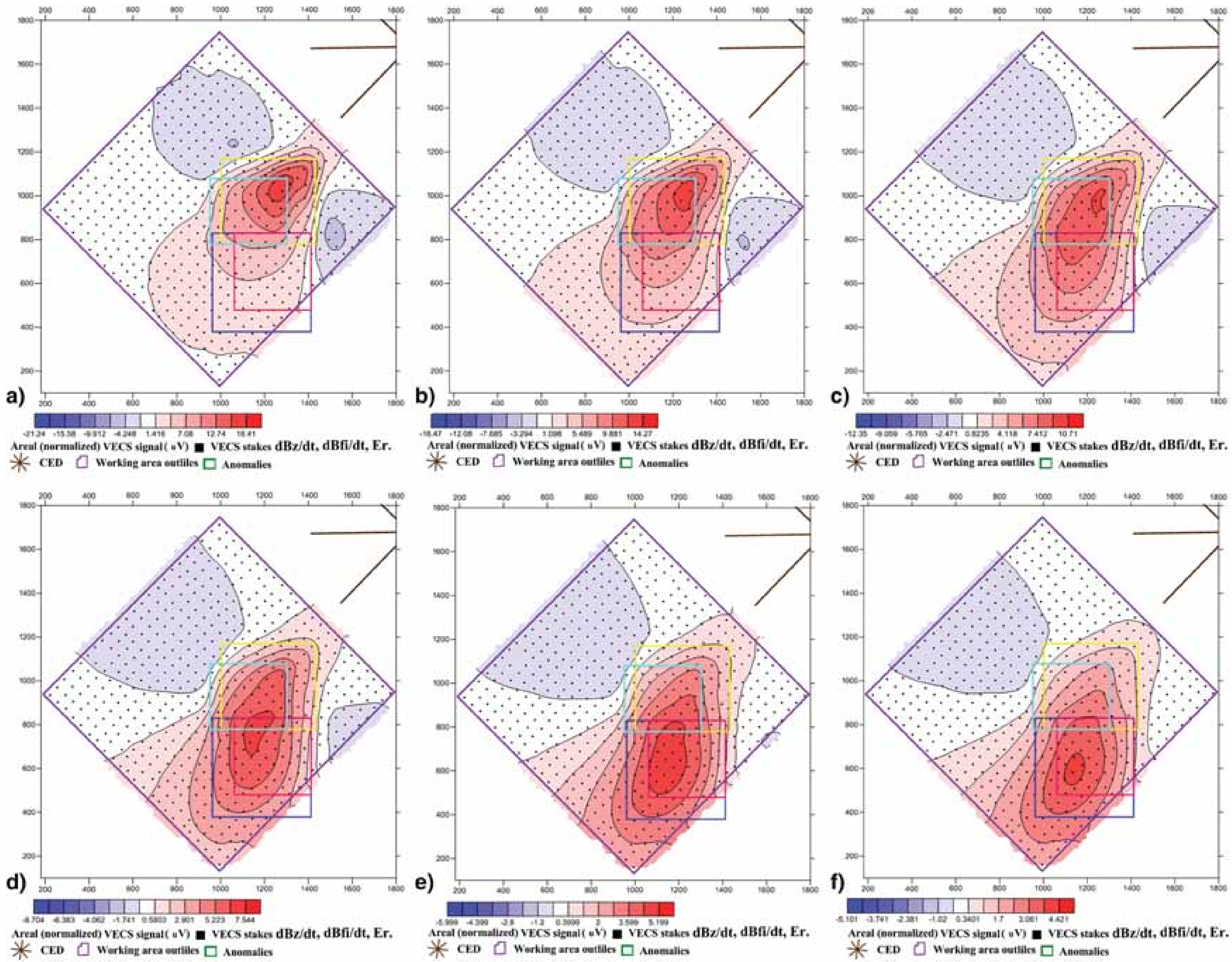

Fig. 18. Areal (normalized) calculation results for preselected model of the $\partial B_{\phi}/\partial t$ component at times a) 0.531 ms, b) 0.795 ms, c) 1.073 ms, d) 1.444 ms, e) 1.943 ms and f) 2.365 ms. Targets at depths 10 m to 30 m, 30 m to 60 m, 60 to 140 m, and 140 m to 500 m are displayed in green, yellow, red, and blue colors, respectively.

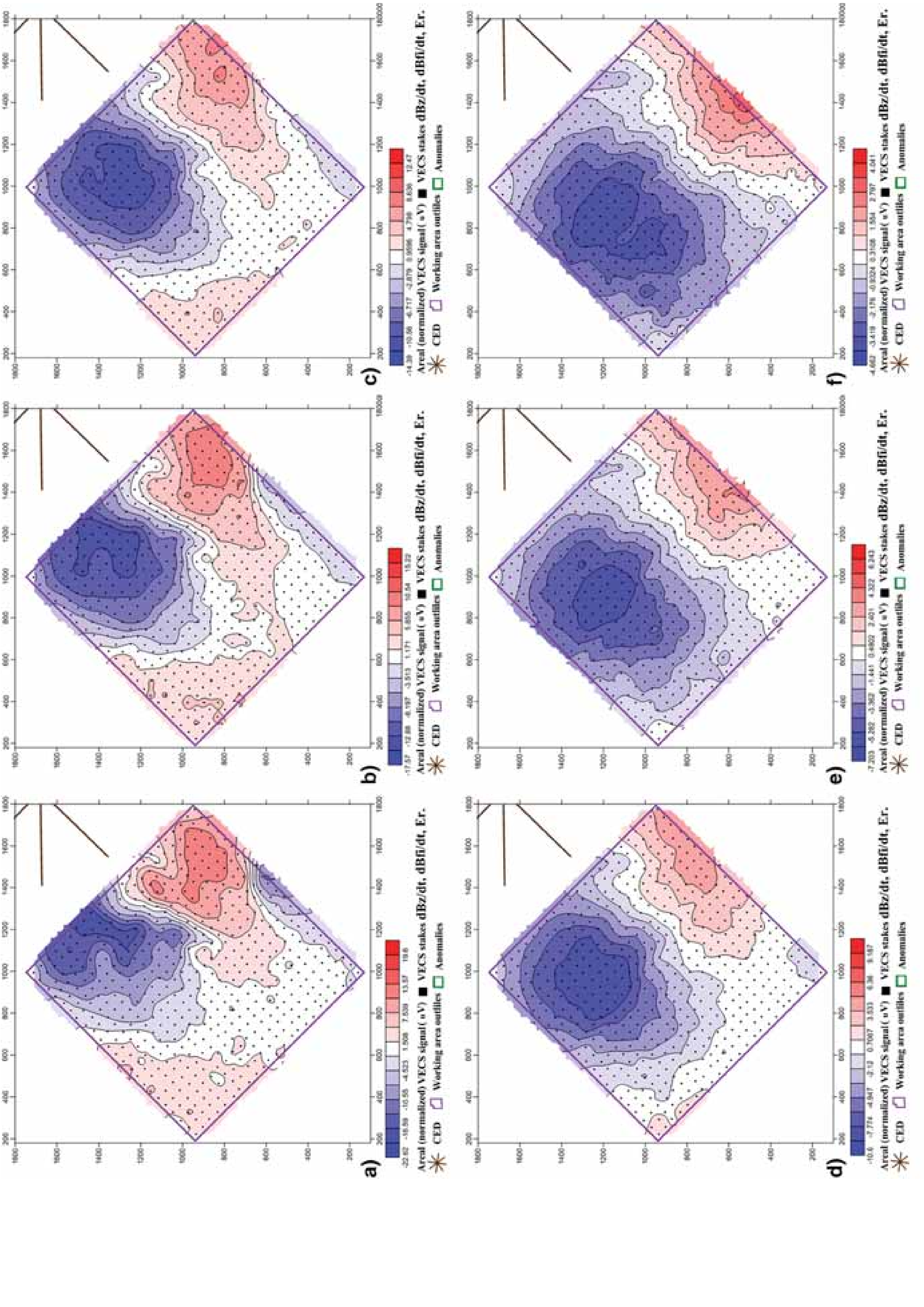

Fig. 19. Areal (normalized) measurement results of the $\partial B_z/\partial t$ component at times a) 0.62 ms, b) 0.849 ms, c) 1.058 ms, d) 1.565 ms, e) 1.965 ms and f) 2.429 ms.

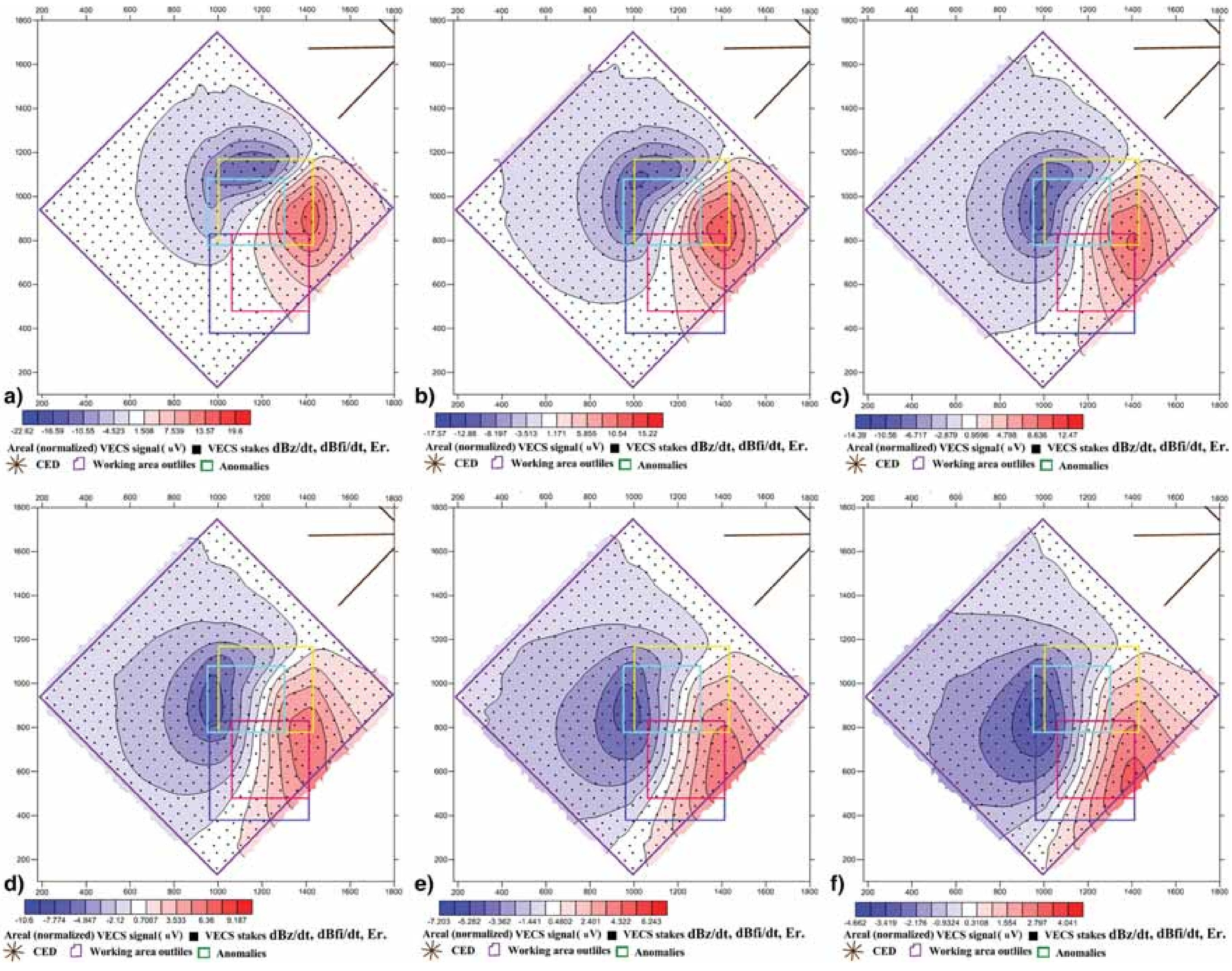

Fig. 20. Areal (normalized) calculation results for selected model of the $\partial B_z/\partial t$ components at times a) 0.531 ms, b) 0.795 ms, c) 1.073 ms, d) 1.444 ms, e) 1.943 ms and f) 2.365 ms. Targets at depths 10 m to 30 m, 30 m to 60 m, 60 m to 140 m, and 140 m to 500 m are displayed in blue, yellow, red, and dark-blue colors, respectively.

Moreover, time at which the maximum anomaly is recorded, also significantly changed. For example, when THREE-DIMENSIONAL simulation is carried out, the second target makes its maximum contribution to a signal at time 300 μs, whereas one-dimensional simulation provides the maximum contribution of the second target at time about 1000 μs.

Given in Fig. 14 are the simulation results of the TEM (coaxial loop-loop) signal for model 3 at two times such as 105 μs and 302 μs. The anomalous signal over the center of the first target accounts for 1% at time 105 μs. The anomalous signal over the center of the second target accounts for 5% at time 302 μs.

Fig. 15 shows the three-dimensional visualization of the $\partial B_\phi/\partial t$ (VECS method) normalized (see Eq. (1)) signal obtained from the calculations results for the third model.

Conclusion:

1) The VECS method. A signal derived from targets of model 3 is steadily measured. Intrusions are distinguished clearly. The signal from targets is well separated in time and space. Targets are steadily singled out in a signal being measured.
2) The TEM method (coaxial loop-loop). A signal derived from the first target of model 005 contributes the anomalous component about 1% into a total signal. A signal derived from the second target of model 005 contributes the anomalous component about 5% into a total signal. It is impossible to visualize targets based on signals inasmuch as such small anomalies will be undistinguishable on the background of changes in a medium of the upper part of the section. At that, the importance of the TEM method for acquisition of the total structural section in the area is validated.

5. Example of field works by VECS method

In what follows, we give results of works by the VECS method in Yakutia. The operation area is comparable with the geological-geophysical situation of model 1. The site of works was a square with sides of 1100 m. Measurements were carried out throughout the dense rectangular survey grid. There were used 23 survey lines, each having 23 measuring points, i.e., 529 measuring points in total. Distances between lines and measurement points on each line was 50 m, i.e., there was a square grid with cells 50*50 m. On the operation area, measurements of a transient characteristic of the $\partial B_\phi/\partial t$ and $\partial B_z/\partial t$ components were performed along the given grid of measurement points. At each point, 2–3 doubles for each component were measured. In addition, in order to acquire information on a host medium, measurements of the E_r component were performed by the VECS method and measurements at 10 points by the TEM with a square loop of 50 m.

It should be said briefly about the provision of facilities for works. When the most of our operations with CED are conducted, we have used the CED composed of eight radial grounded horizontal current lines. When the present works were carried out, the CED radius was 450 m. We usually use the ZaVeT system developed and produced by us. Current is the same in all eight lines, this being controlled in an automated mode by the ZaVeT equipment, which allows the total current to be set in the range from 4 A to 160 A. The current stability and scatter of current values in lines is within 1%. For measurement of transient signals, common meters for transient processes were used. In the present investigations, compact inductive pickups with the effective area of 10,000 m^2 (produced by the ZaVeT-GEO Company) were used.

Data processing is executed using programs ZaVeT-M, Podbor, Vybor-TS, and GeoPrep. The set of these programs permits the operator to process, normalize, and visualize VECS data and data of traditional methods of transient sounding, to perform one-dimensional simulation of signals generated by an arbitrary source with arbitrary current pulse taking into account polarization parameters and medium anisotropy. For the three-dimensional simulation of transient electromagnetic methods, the Podbor program was used. Calculations of 3D models in the Podbor program are based on the Born approximation. For 3D

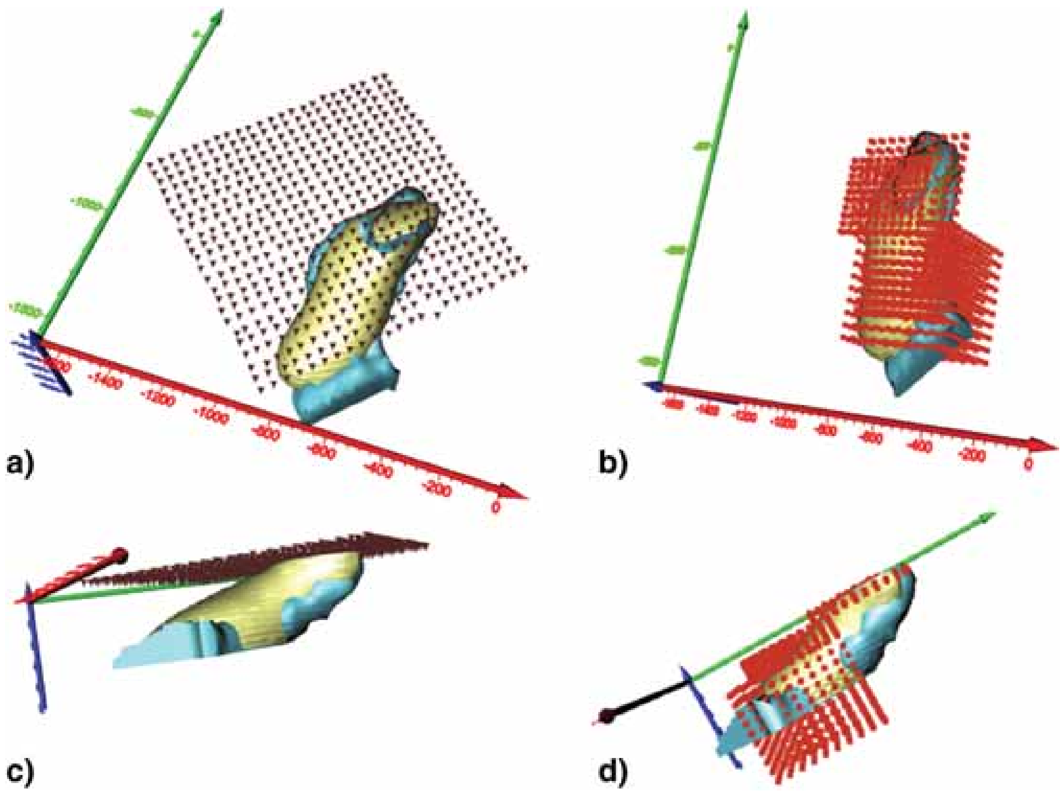

Fig. 21. The 3D visualization of a field $\partial B_\phi/\partial t$ signal and a signal acquired from calculations for the fitted model. The field $\partial B_\phi/\partial t$ signal with due regard to the local topography is displayed in blue color, the $\partial B_\phi/\partial t$ signal calculated for the fitted model is displayed in yellow color, and the fitted model is displayed as a set of orange points.

simulation of the VECS method, we applied the GeoPrep program, the finite element method is used in the program (Persova et al., 2011). First the TEM data were processed. The aim was acquisition of data on a host medium, which further would be used for three-dimensional interpretation of VECS results using the data of measured magnetic components. Subsequently, the data of the measured E_r component of the VECS method were interpreted; inversion was carried out within the framework of one-dimensional model. Acquisition of data on a host medium was also the aim of the work. When field data of measured magnetic components $\partial B_\phi/\partial t$ and $\partial B_z/\partial t$ were obtained, areal signals at specified times with their normalization depending on the distance from a source were constructed. In addition, apparent sections in which the time was transformed into depths via the equation for skin-layer were constructed. Using the entire three-dimensional data cube, we constructed three-dimensional images of the target being studied. When processing the data, we solve the inverse problem by means of three-dimensional mathematical simulation and fitting local targets. As a result of these works, a three-dimensional model was constructed, calculated signal from this model corresponded to the field signal. The results of works by the transient electromagnetic method are given in Fig. 16, which shows the survey line, along which measurements were performed, and the results of transformation of signals into apparent resistivities, as well as results of one-dimensional interpretation. According also to the results of one-dimensional interpretation the apparent resistivity varied within ranges from 45 to 65 Ω∗m. Based on the results of works using the TEM (coaxial loop-loop), we acquired data on depths from 50 to 300 m. According to the results of one-dimensional interpretation of the E_r component for the VECS method, we obtained the three-layer model of a medium with resistivities of the first and second layers to be 150 Ω∗m and 5 Ω∗m and thicknesses 350 m and 30 m. The basement resistivity was determined as 1000 Ω∗m. Thus, when conducting these works, the resistivity of the first layer was 50 Ω∗m determined by the TEM was 50 Ω∗m, the resistivity of the first layer determined by the VECS method was 150 Ω∗m, i.e., there was the three-time difference. Such, at first sight, paradoxical result is due to the fact that the TEM determines only a horizontal resistivity, whereas both vertical and horizontal resistivities affect VECS processes. When interpreting magnetic components by the VECS method, we get strong differences also in anomaly resistivities determined by TEM and VECS.

Fig. 17 shows areal (normalized see Eq. (1)) measurements of the $\partial B_\phi/\partial t$ components at times 0.545 ms, 0.780 ms, 1.058 ms, 1.431 ms, 1.965 ms, and 2.429 ms. Outlines of the first and second targets selected as the initial approximation are displayed on the plan in green color. Prior to fitting a form of a geological heterogeneity, we singled out two zones where signals were strongest. The first zone of strongest signals was revealed at times 0.545 ms, 0.780 ms, and 1.058 ms and it corresponded to the target located closer to the earth's surface. The second zone of strongest signals was revealed at times 1.965 ms and 2.429 ms and it corresponded to the deeper target. We also took into account that with increasing time, the signal maximum would not be over the target center, but some further from the CED center. We assumed that a signal at time 1.431 ms should be in the intermediate position between the first and second zones. With respect to these zones, we inferred two targets corresponding to the first and second zones. After preliminary calculations, we inferred the first target to be at the depth from 10 to 60 m and the second target to be at the depth from 60 to 500 m. The selected targets are shown in Fig. 18.

Fig. 18 demonstrates the distribution of a calculated normalized (see Eq. (1)) signal for a fitted target model, the $\partial B_\phi/\partial t$ components being at different times. In Fig. 18, view plans of targets which made up a target model are given: targets at depth 10 m to 30 m, 30 m to 60 m, 60 to 140 m, and 140 m to 500 m are displayed in green, yellow, red, and blue colors, respectively. The calculations showed that we got data on the medium to about 300 m. As it can been seen from the fitted model, target depths changed a little and the locations of the target were also changed. Nevertheless, positions of the targets preselected in conformity with the field data proved to be good as an initial approximation.

Having fitted a model with respect to the $\partial B_\phi/\partial t$ component, we checked the results with respect to the $\partial B_z/\partial t$ component. In Fig. 19, the areal (normalized see Eq. (1)) measurements of the $\partial B_z/\partial t$ component with due regard to the local topography are shown. In Fig. 20, areal (normalized see Eq. (1)) calculation results for the fitted model of the $\partial B_z/\partial t$ component at various times are displayed in blue, yellow, red, and dark-blue colors for depths 10 m to 30 m, 30 m to 60 m, 60 to 140 m, and 140 m to 500 m, respectively. No contradictions were revealed in the simulation results of signals being observed. The signals of the $\partial B_z/\partial t$ component fully confirmed our inferences that the fitted model completely agree with field signals.

In Fig. 21, the 3D visualization of the field $\partial B_\phi/\partial t$ signal and the signal acquired from calculations for the fitted model is given. The field $\partial B_\phi/\partial t$ signal with due regard of the local topography is displayed in blue color, the $\partial B_\phi/\partial t$ signal calculated for the fitted model is displayed in yellow color, and the selected model is displayed as orange points.

The results of the present works are as follow:

1) According to the TEM data, the resistivity of a host medium is about 50 Ω∗m and the pipe resistivity is usually about 40 Ω∗m. Due to the low contrast between horizontal resistivities of the host medium and the pipe being studied, small target area, and the great cover thickness, pipes are not distinguishable by 'classical' methods of electrical exploration.
2) Based on the results of 1D inversion of E_r signals, we have determined resistivity of the first layer of the host medium as 150 Ω∗m, that is two-three times greater than resistivity of the host medium according to the TEM results. Increase in the host medium resistivity determined by the VECS method is explained by the fact that when working with vertical currents, the vertical resistivity plays significant role, whereas when working with a source of the loop type, only the horizontal resistivity takes place.
3) The pipe is well manifests itself in VECS signals. We were able to distinguish two targets with respect to $\partial B_z/\partial t$ and $\partial B_\phi/\partial t$ components, which are located in the immediate vicinity from each other (distance between their centers is about 300 m) and they even partly overlap each other.
4) We have executed the comprehensive inversion using forward problems of 3D simulation. Despite a low contrast between resistivity of a host medium and that of a target being studied by "classic" methods, the target was well manifested when works were performed by the VECS method and also due to the high contrast in vertical resistivities between the target and host medium.
5) The host medium resistivity determined by VECS method was found to be higher than that by the TEM, and the target resistivity was lower than it usually was for such targets in this region. That is, we revealed the higher contrast between resistivities of the host medium and target than it was specific for the 'classical' TEM. In practice, it leads to the fact, that we record signals 10–50 times greater that it was expected. In practice of electrical exploration by 'classical' methods, the reverse situation is more common: a field anomalous signal is usually several-fold lower than it was expected when simulation was conducted before field works.

6. Discussion and conclusion

Surveying by the VECS as applied to ore targets has, from our point of view, a number of features and advantages:

- Medium heterogeneities with respect to resistivity are manifested themselves in the CED field much stronger that those when a horizontal line or loops are used. Signals calculated for such resistivity model when CED is used usually exceed the calculated ones 10–50 times. This is associated with several circumstances, but before all, with the fact that resistivities of targets and a host medium are, as a rule, have been determined based on date acquired by operations applying the TE field or geophysical logging data. When data of previous works are used, the contrast in vertical resistivity is not taken into account, whereas the contrast in resistivity is always recorded lower than it actually is.

- Received signals ($\partial B_z/\partial t$ and $\partial B_\phi/\partial t$) are governed by heterogeneities near measurement points inasmuch as an anomalous field is complete. In the case when a horizontal line or a current loop is applied, signals are often governed mainly by a host medium. It is difficult to distinguish local information in this total signal. Rather complex signal processing is required. When a common one-dimensional approach to interpretation is applied at the first stage, the information will be completely eliminated.
- Measured signals from different electromagnetic field components compliment to each other well and allow anomalies revealed by measurements of individual components to be rejected.
- When surveying with a circular electric dipole, it makes sense to condense a survey grid to the required accuracy of determination of target boundaries. When surveying with a loop or a horizontal line, condensation of survey grid is unsuccessful since the signal variation is primarily associated with a change in response of one-dimensional medium depending on the distance between generator and measurement point. When surveying by the VECS method, the procedure with condensation of a survey grid at sites, where a target signal is recorded, is the standard procedure.
- The economic efficiency is also takes place. When surveying with CED, the fixed source is once set to cover a whole area being studied. For generation of a dense survey grid in TEM, the entire receiver-current circuit is required to be moved over the area.
- VECS realizes the long-held dream of electrical explorationist to separate the signal being measured into transient and polarization signals. The signal separation will allow us to study resistivity variations of a medium and change in polarization parameters. Based on measurements of magnetic components, we study resistivity of a medium including local three-dimensional inclusions. Based on measurements of electric components, we study polarization parameters of a medium just having insight about the resistivity distribution in the medium.

If the 'classic' TE-geoelectrics have given no results, try to make use of the TM-electrical exploration before you pull the plug on electrical exploration.

References

Balashov, B.P., Mukhamadiev, R.S., Mogilatov, V.S., Andreev, D.S., Zlobinskiy, A.V., Shishkin, V.K., Stogniy, V.V., 2011. Vertical electric current soundings for hydrocarbon exploration. Geofizika 1, 61–66 (in Russian).

Goldman, M., 1990. Non-conventional method in geoelectrical prospecting. Ellis Horwood Series in Applied Geology (153 pp).

Goldman, M.M., Mogilatov, V.S., 1978. Transient electromagnetic process of the vertical electric dipole embedded in a horizontally-layered half-space. Theory and Experience of Applying Electromagnetic Fields in Exploration Geophysics. Proceedings of Institute of Geology and Geophysics SB USSR Academy of Sciences, Novosibirsk, pp. 123–138 (in Russian).

Goldman, M., Mogilatov, V., Haroon, A., Levi, E., Tezkan, B., 2015. Signal detectability of marine electromagnetic methods in the exploration of resistive targets. Geophys. Prospect. 63, 192–210.

Haroon, A., Goldman, M., Mogilatov, V., Bergers, R., Tezkan, B., 2016. Exploration of resistive targets within shallow marine environments using the Circular Electrical Dipole and the Differential Electrical Dipole methods. A time-domain modelling study. Geophys. J. Int. 205 (2), 1032–1048.

Helwig, S.L., Mogilatov, V.S., Balashov, B.P., 2010. The use of a circular electrical dipole source in hydrocarbon exploration. 80th Annual International Meeting, SEG, Expanded Abstracts 29, p. 764.

Helwig, Stefan L., Wahab, El Kaffas Abdul, Terje, Holten, Oyvind, Frafjord, Kjetil, Eide, 2013. Vertical dipole CSEM: technology advances and results from Snohvit field. First Break 31 (4), 63–68.

Mogilatov, V., 1996. Excitation of a half-space by a radial current sheet source. Pure Appl. Geophys. 147 (4), 763–775.

Mogilatov, V., 2014. Pulse Geoelectrics. Novosibirsk State University, Novosibirsk (182 pp).

Mogilatov, V., Balashov, B., 1996. A new method of geoelectrical prospecting by vertical electric current sounding. J. Appl. Geophys. 36, 31–41.

Mogilatov, V., Mukhopadhyay, P., Mallick, S., 2009. An advanced deep penetrating EM technique for hydrocarbon and mineral exploration: mVECS. NGF Abstracts and Proceedings vol. 3, pp. 21–24.

Mogilatov, V., Goldman, M., Persova, M., Soloveichik, Y., Koshkina, Y., Trubacheva, O., Zlobinskiy, A., 2016. Application of the marine circular electric dipole method in high latitude Arctic regions using drifting ice floes. J. Appl. Geophys. 135, 17–31.

Mogilatov, V., Zlobinskiy, A., Balashov, B., 2017. Transient electromagnetic surveys with unimodal transverce magnetic (TM) field: ideas and results. Geophys. Prospect. 5 (5), 1380–1397.

Nabighian, M.N., 1979. Quasi-static transient response of a conducting half-space – an approximate representation. Geophysics 44, 1700–1705.

Nazarenko, O., 1962. Device for marine electrical. Certificate of Authorship No 150184 (in Russian).

Park, J., Lee, K.-H., Seo, H., Ryu, J., Lee, I.-M., 2017. Role of induced electrical polarization to identify soft ground/fractured rock conditions. J. Appl. Geophys. 137 (February), 63–72.

Persova, M.G., Soloveichik, Y.G., Trigubovich, G.M., 2011. Computer modeling of geoelectromagnetic fields in three-dimensional media by the finite element method. Izv. Phys. Solid Earth 47 (2):79–89. https://doi.org/10.1134/S1069351311010095.

Seidel, M., Tezkan, B., 2017. 1D Cole-Cole inversion of TEM transients influenced by induced polarization. J. Appl. Geophys. 138 (March), 220–232.

Zlobinskiy, A.V., Mogilatov, V.S., 2014. Electrical prospecting by the VECS method in ore geophysics. Geofizika 1, 26–35 (in Russian).